Observation of Nuclear Magnetic Order in Solid ^{3}He†

W. P. Halperin, C. N. Archie, F. B. Rasmussen,* R. A. Buhrman, and R. C. Richardson
Laboratory of Atomic and Solid State Physics,
Department of Applied Physics, Cornell University, Ithaca, New York 14850
(Received 11 March 1974)

Measurements of $T\,dP/dT$ have been made along the ^{3}He melting curve near an anomaly at $T_s = 1.17$ mK. It is found that the solid-^{3}He entropy decreases by 80% in an interval of 100 μK at T_s. This is attributed to onset of nuclear magnetic order.

In the past decade there has been considerable interest[1] in the prediction of properties of the magnetically ordered nuclear spin state expected in solid ^{3}He. In this work, we have discovered that the magnetic entropy of the solid decreases from $0.5R\ln 2$ to $0.1R\ln 2$ in an interval of 100 μK at a temperature $T_s = 1.17$ mK. We interpret this result as evidence of a nuclear magnetic phase transition in solid ^{3}He at T_s.

This effect was first seen while the solid was being formed at a constant rate in a Pomeranchuk cell.[2] We observed that the compressional cooling rate, as indicated by a pressure gauge, decreased abruptly at a melting-curve pressure $P_s = 34.394$ bar, a pressure 52.3 ± 0.2 mbar higher than P_A, the melting pressure of the A transition in the liquid phase. Subsequently, we have been able to calculate the temperature variation of the solid entropy near T_s from measurements of the latent heat of solidification.

Our Pomeranchuk cell is described in a previous paper.[3] The ^{3}He was contained in a pancake-shaped region directly below a 3.81-cm-diam Be-Cu diaphragm, 7.4×10^{-2} cm thick. Displacement of the diaphragm by increasing the pressure on the liquid ^{4}He in the upper part of the cell produced the volume change required for the adiabatic solidification of the ^{3}He. Volume changes were determined by a capacitance measurement of the displacement of the compression diaphragm. The pressure of the ^{3}He was indicated by a Straty-Adams-type[4] capacitance gauge situated in the cell wall below the ^{3}He. Volume and pressure calibrations were made to an accuracy of 1 and 0.01%, respectively, and are discussed in detail elsewhere.[5] A 3-m length of No. 52 copper heater wire was woven in a web uniformly distributed throughout the sample region. This heater was joined to a pair of superconducting wires that led out of the cell. The heater power was measured with a four-terminal technique to an accuracy of 0.3%. The ^{3}He volume was 4.34 cm^3 with 0.169 moles of liquid just pressurized to the melting curve at the precool temperature of 19 mK. For a typical experiment 22% of the sample was solidified in a 1-h pressurization to reach P_s. A further 40% solid was generated at pressures near P_s during the course of the measurements.

In studies along the low-temperature melting curve it was found that the different thermal time constants of the liquid and solid ^{3}He permit separate analysis of the two phases. The liquid along with the layer of solid ^{3}He at the phase interface forms one equilibrium thermodynamic system. The effect of the solid phase within the cell is to cause either a positive or negative heat leak into that system, depending upon the relative temperatures of the two phases. Following a 0.5-sec heating or cooling pulse, *all* of the resultant heating or cooling occurs in the system consisting of the liquid and the liquid-solid interface. This conclusion is based upon the following observations: (a) A heat pulse is always immediately followed by a pressure decrease. (b) After the pulse, the characteristic time for establishment of the lower melting pressure is 6 sec at 20 mK and less than 0.1 sec at 1 mK. (c) The magnitude of the pressure change corresponds to a temperature change given by the heat capacity of the liquid fraction in the cell and the amount of heat in the pulse. (d) An abrupt increase in the ^{4}He pressure (a cooling pulse) produces an immediate increase in the ^{3}He pressure for which the same equilibrium times are seen as for heating pulses. (e) All of the above results are independent of the amount of solid in the cell.

We have measured the thermal equilibrium time for the bulk solid to be 14 min at 2 mK and 3 min at 8 mK. Therefore, the bulk solid will manifest itself only as a slowly varying heat load on the interface-liquid system. These results are consistent with an extrapolation of NMR

relaxation measurements to these temperatures.[6] As the temperature is decreased there is a rapid deterioration in the efficiency of the mechanisms coupling the lattice to the exchange-energy reservoir. Thus, phonons generated in a heat pulse leak out of the solid lattice before the spin temperature is perturbed.

In the compressional cooling process we reduce the cell volume at a rate $\dot{V}$, thereby solidifying ^{3}He at a rate $-\dot{n}_l$ given by $\Delta v \dot{n}_l = \dot{V} + \dot{P}(\kappa_l V_l + \kappa_s V_s)$; here $\Delta v = 1.314$ cm^3 mole^{-1} is the molar volume difference between liquid and solid,[5] n_l is the number of moles of liquid, P is the ^{3}He pressure, and κ_l, κ_s, V_l, and V_s are the respective compressibilities and volumes of the liquid and solid ($V = V_l + V_s$). Using the Clausius-Clapeyron equation, where s denotes the molar entropy, the cooling power $T(s_s - s_l)\dot{n}_l$ can be written as $T(dP/dT)\Delta v \dot{n}_l$. If this quantity is larger than $\dot{Q}$, the sum of applied heat and heat leak including the effective heat leak from the solid, then the liquid will cool and the pressure will increase along the melting curve at a rate

$$\dot{P} = -(dP/dT)[T(dP/dT)\dot{n}_l \Delta v - \dot{Q}]n_l^{-1}c_l^{-1}, \quad (1)$$

where c_l is the molar specific heat of the liquid, and dP/dT is the slope of the melting curve. When pressure equilibrium is established, $\dot{P} = 0$, and Eq. (1) yields

$$\dot{Q}/\dot{V} = dQ/dV = T\,dP/dT. \quad (2)$$

Since $s_s \gg s_l$, this quantity is dominated by the behavior of the solid entropy and can be found from measurement of heat and volume at constant pressure.

In Fig. 1, the four pressurization traces illustrate different experiments performed near T_s. The rates of solid formation and the quantities of heat added are indicated. In the trace labeled a the compression rate was not sufficient to produce cooling below the transition. The traces b and c show three different methods of measuring $T\,dP/dT$ at T_s and lower temperatures:

(1) Trace b demonstrates how a stepped increase in the solidification rate $\dot{n}_s$ resulted in a stepped increase in the melting pressure, and hence lower temperature than T_s. Assuming that the heat leak is constant, and calibrating it above T_s, we obtain [using Eq. (2)] the values of $T\,dP/dT$ versus $P_s - P$ shown by the squares in Fig. 2.

(2) In trace c we opposed the effect of an increased $\dot{n}_s$ by applying the heater power $\dot{Q}_a$; 1 min of heating was sufficient to establish a higher stable temperature (lower pressure). In this case $\dot{Q}_a/\dot{V}$ is shown by the solid triangles in Fig. 2. The heat leak is neglected in this procedure.

(3) When $\dot{Q}_a$ is switched off, the liquid instant-

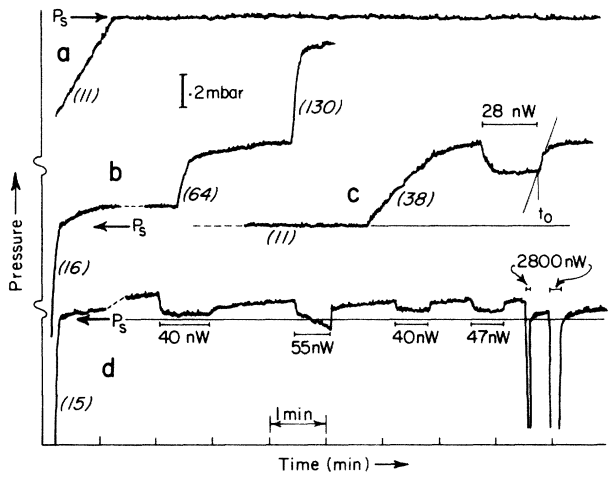

FIG. 1. Four pressurization traces. P_s is the melting pressure of the solid transition. The solidification rate is indicated in parentheses (in units of μ mole sec^{-1}). Any changes in this rate are made in discontinuous steps. The dashed lines show interrupted traces, i.e., c is a continuation of a. When heat is applied the power is shown (in nanowatts) beside the appropriate time interval.

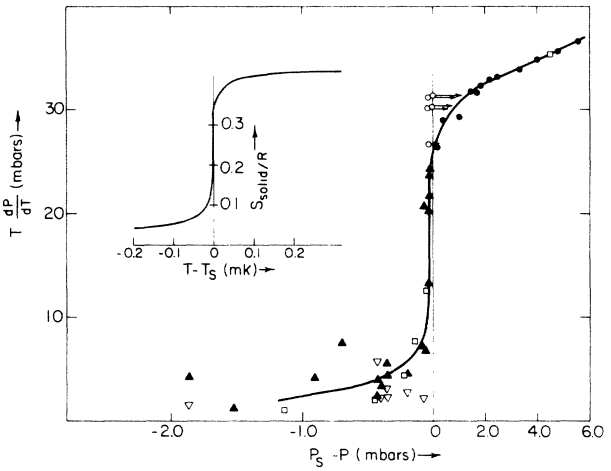

FIG. 2. The cooling capacity; $T\,dP/dT$ versus $P_s - P$. Note the change in pressure scale on either side of zero. A detailed explanation for each set of points is given in the text. Inset, temperature variation of the solid entropy derived from the line drawn through the data.

ly starts cooling again at a rate $\dot{P}_0$ determined by Eq. (1). In this third method we explicitly account for the heat leak by comparing $\dot{P}$ just before and after the applied heat $\dot{Q}_a$ is turned off at t_0. For the trace shown, $\dot{P}=0$ before t_0; after the switching, the value of the expression in brackets in Eq. (1) changes from 0 to $\dot{Q}_a+\dot{P}_0(\kappa_l V_l + \kappa_s V_s)T\,dP/dT$. Solving Eq. (1) for $T\,dP/dT$ we obtain the inverted open triangles shown in Fig. 2.

Figure 1, trace *d*, shows an experiment performed at constant compression rate at pressures close to P_s. Increases of heating in the ^{3}He caused small pressure decreases close to P_s. When, at this compression rate, sufficient heat was applied (0.55 erg sec^{-1}), the ^{3}He warmed through P_s and would have continued to warm until a melting pressure was reached such that

$$\frac{T\,dP}{dT} = \frac{0.55 \text{ erg sec}^{-1}}{15\ \mu\text{mole sec}^{-1}}\,\Delta v$$

if a sufficient time were allowed. Points such as these, where a constant temperature was not established, are plotted as open circles with arrows in Fig. 2. It is expected that changes in the thermal conductivity and specific heat of the solid will alter the heat load on the liquid-interface system. In method (1) this heat leak is assumed to be constant, in method (2) it is neglected, and in method (3) it is explicitly included in the analysis. A comparison of these results shows that this effect is sufficiently small that to within a factor of 2 the magnitude of $T\,dP/dT$ below T_s can be represented by a curve such as that drawn through all of the data.

A more accurate measurement of $T\,dP/dT$ is possible at temperatures higher than T_s where the cooling power allows us to keep the temperature constant using a very small $\dot{n}_s$. Here, we regulate the compression rate by means of an automatic feedback system to keep the cell pressure, and hence the temperature of the liquid, constant. When a heat pulse ΔQ is applied, the feedback system changes the volume ΔV, and $T\,dP/dT$ can be calculated directly from Eq. (2). The closed circles in Fig. 2 at temperatures above T_s were all obtained in this way. Measurements of this type, affording a precision better than 1%, have been carried out up to 23 mK. Analysis of these measurements[5] gives $T_s = 1.17$ mK $\pm$ 6%.

We attribute the scatter in the results below T_s shown in Fig. 2 to uncertainties in the pressure measurement during rapid compression and to difficulties in establishing the same conditions (i.e., configuration of solid) in successive experiments.

From the solid line drawn in Fig. 2 and the expression

$$T/T_s = \exp\left[\int_{P_s}^{P}(T\,dP'/dT)^{-1}\,dP'\right],$$

we have calculated the temperature scale near T_s and hence the solid entropy shown in the inset. The transition is either a narrow second-order transition or a first-order transition. The precursory behavior suggested by the rounding of the entropy curve above T_s favors the former.

In conclusion, we have observed that less than 8% of the $R\ln 2$ magnetic entropy remains in the solid below 1 mK, following a narrow, nonhysteretic transition at 1.17 mK. It is not possible to deduce from our data which type of magnetic order characterizes solid ^{3}He below T_s. A high-temperature expansion of a simple Heisenberg-model Hamiltonian with nearest-neighbor exchange energy given by $J/k = -0.8$ mK has been found to fit a number of experiments[1,7-9] performed in zero magnetic field at temperatures above 6 mK. The model predicts an antiferromagnetic spin ordering at 2.2 mK. The model has previously been found to be inconsistent both with measurements of thermal expansion of the solid in large magnetic fields,[10] and with the large nuclear magnetic susceptibilities at low temperatures reported by Osheroff, Richardson, and Lee.[11] In this work the model is inconsistent with the observation of the transition at half of the expected temperature. Although an improved theory including triple exchange can account for the thermal expansion data, it only increases the estimate of the transition temperature.[12] In view of the serious failures of the model at low temperatures, the nature of the solid magnetization below T_s remains an open question.

We gratefully acknowledge useful conversations with Professor J. W. Wilkins, Professor M. E. Fisher, Professor J. D. Reppy, Professor D. M. Lee, Dr. A. K. McMahan, and Dr. W. S. Truscott.

†Research supported by the National Science Foundation under Grant No. GH-38785 and by the Cornell Materials Science Center through the National Science Foundation Grant No. 33637.

*On leave from the Ørsted Institute, University of Copenhagen, 2100 Copenhagen, Denmark.

[1]S. B. Trickey, W. P. Kirk, and E. D. Adams, Rev. Mod. Phys. 44, 668 (1972).
[2]W. P. Halperin, R. A. Buhrman, and R. C. Richardson, Bull. Amer. Phys. Soc. 18, 642 (1973).
[3]W. P. Halperin, R. A. Buhrman, W. W. Webb, and R. C. Richardson, in *Low Temperature Physics, LT-13*, edited by W. J. O'Sullivan, K. D. Timmerhaus, and E. F. Hammel (Plenum, New York, 1973).
[4]G. C. Straty and E. D. Adams, Rev. Sci. Instrum. 40, 1393 (1969).
[5]W. P. Halperin, C. N. Archie, F. B. Rasmussen, R. A. Buhrman, and R. C. Richardson, to be published.
[6]R. A. Guyer, R. C. Richardson, and L. I. Zane, Rev. Mod. Phys. 43, 532 (1971).
[7]M. F. Panczyk and E. D. Adams, Phys. Rev. 187, 321 (1969).
[8]W. P. Kirk, E. B. Osgood, and M. Garber, Phys. Rev. Lett. 23, 833 (1969); J. R. Sites, D. D. Osheroff, R. C. Richardson, and D. M. Lee, Phys. Rev. Lett. 23, 836 (1969).
[9]S. H. Castles and E. D. Adams, Phys. Rev. Lett. 30, 1125 (1973).
[10]W. P. Kirk and E. D. Adams, Phys. Rev. Lett. 27, 392 (1971).
[11]D. D. Osheroff, R. C. Richardson, and D. M. Lee, Phys. Rev. Lett. 28, 885 (1972).
[12]L. I. Zane, J. Low Temp. Phys. 9, 219 (1972); A. K. McMahan and R. A. Guyer, Phys. Rev. A 7, 1105 (1973); E. D. Adams and L. H. Nosanow, J. Low Temp. Phys. 11, 11 (1973).

Magnetothermal Resistivity of Potassium*

R. Fletcher
Physics Department, Queen's University, Kingston, Ontario, Canada
(Received 10 December 1973)

This Letter reports the results of an investigation of the magnetothermal resistivity of potassium aimed at measuring the contribution of the lattice to the thermal current. The observed behavior of the lattice conductivity is contrary to that expected, possibly suggesting other contributions to the thermal current.

If one assumes that the electronic thermal conductivity tensor $\overleftrightarrow{\lambda}_e$, in the presence of a magnetic field along the z axis, is of the form

$$\overleftrightarrow{\lambda}_e = \begin{vmatrix} \lambda_{xx} & \lambda_{xy} & 0 \\ -\lambda_{xy} & \lambda_{xx} & 0 \\ 0 & 0 & \lambda_{zz} \end{vmatrix}$$

and that the phonon conductivity is simply $\lambda_g \overleftrightarrow{I}$, where $\overleftrightarrow{I}$ is a unit matrix, then taking the thermal resistivity $\overleftrightarrow{\gamma}$ to be the inverse of $\overleftrightarrow{\lambda}_e + \lambda_g \overleftrightarrow{I}$ and assuming thermoelectric terms to be negligible one can show[1] after some manipulation that the measured transverse thermal resistivity $\gamma_{xx}{}^m$ measured under the condition $\partial T/\partial y = 0$ is given by

$$\gamma_{xx}{}^m = \gamma_{xx}{}^e \left(\frac{\alpha + \lambda_g (\gamma_{yx}{}^e)^2 (\gamma_{xx}{}^e)^{-1}}{\alpha^2 + (\lambda_g \gamma_{yx}{}^e)^2} \right).$$

In this equation $\gamma_{xx}{}^e$ and $\gamma_{yx}{}^e$ are the transverse and Righi-Leduc thermal resistivities that the electrons would exhibit if $\lambda_g = 0$, and $\alpha = (1 + \gamma_{xx}{}^e \lambda_g)$. For uncompensated metals in not too high fields the equation reduces, to an excellent approximation, to

$$\gamma_{xx}{}^m = \gamma_{xx}{}^e + (\gamma_{yx}{}^e)^2 \lambda_g. \quad (1)$$

It is also possible to show, with the same assumptions, that $\gamma_{yx}{}^e$ differs insignificantly from the measured value $\gamma_{yx}{}^m$ so that Eq. (1) provides a simple and convenient method of obtaining λ_g. Potassium is an excellent material for study since it can be obtained with high purity (thus $\gamma_{xx}{}^e$ is small) and $\gamma_{yx}{}^m$ is large.[2] We report here our investigations, prompted by the aforegoing predictions, on $\gamma_{xx}{}^m$ for several samples of pure potassium.

All the samples were obtained from Mine Safety Appliances Ltd.[3] The preparation and handling of similar samples has already been outlined,[2] but in the present case there are some modifications. The samples were approximately $50 \times 4 \times 1$ mm^3 in size and were cut from a rolled sheet using a simple sharp-edged mold. Limbs were provided to measure the longitudinal temperature difference ΔT_l appropriate to $\gamma_{xx}{}^m$ and, in the case of sample No. 3 (K3) only, transverse limbs were incorporated to determine the temperature difference appropriate to $\gamma_{yx}{}^m$. Heater powers of 1–10 mW produced $\Delta T_l/T \sim 0.2$–0.5%, T being the mean temperature of the sample. The small ΔT were determined with carbon thermometers using ac excitation powers of 1 nW at 4 K decreasing to 30 pW at 1.5 K; these showed magnetoresistance